



**LIGO**: The Laser Interferometer Gravitational-wave Observatory

*General Relativity...*

*A new window...*

*Einstein...*

*Astrophysics...*



# Gravitational Waves and the R-modes

Gregory Mendell

LIGO Hanford Observatory



# Who's Involved?

Caltech, MIT, and the LIGO Science Collaboration

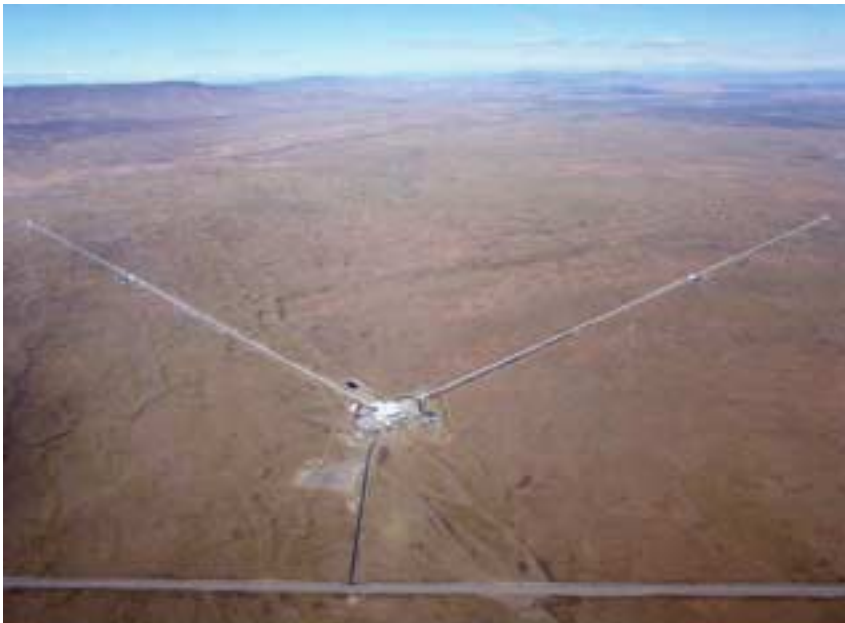
The image shows a screenshot of a Microsoft Excel spreadsheet. The spreadsheet contains a table with the following columns: Institution, Heads, FTE, Heads, FTE, Heads, and FTE. The data is organized into several groups of institutions, with a total row at the bottom. The total row shows 229 Heads and 163.8 FTE for Non-LIGO Laboratory, 134 Heads and 84.4 FTE for LIGO Laboratory, and 132 Heads and 79.4 FTE for the total.

Institution	Heads	FTE	Heads	FTE	Heads	FTE
ACIGA	21	13.5	0	0.0	21	13.5
Caltech - CACR	3	0.7	3	0.7	0	0.0
Caltech - CaRT	6	3.1	1	0.4	1	2.7
Caltech - CEGG	2	1.6	1	0.3	2	1.3
Cal. State Dominguez Hills	5	4.6	5	4.6	0	0.0
Carleton University	1	0.8	1	0.8	0	0.0
Cornell	3	2.6	3	2.6	0	0.0
GEO 600	58	47.0	49	30.4	32	16.6
Harvard-Smithsonian	2	1.3	2	1.3	0	0.0
Inst. of Applied Physics - Russia	11	7.0	0	0.0	11	7.0
Inter-University Centre for Astronomy and Astrophysics (India)	5	2.2	5	2.2	0	0.0
Iowa State University	1	0.5	0	0.0	1	0.5
JILA (Univ. of Colorado)	5	1.5	0	0.0	5	1.5
Louisiana Tech	4	1.2	4	1.2	0	0.0
LSU	10	5.5	9	4.0	6	1.5
Moscow State University	9	9.0	0	0.0	9	9.0
NAOJ - TAMA	5	2.0	0	0.0	5	2.0
Oregon University	7	4.1	7	4.1	0	0.0
Penn State	14	13.3	10	8.8	8	4.7
Southern Univ/AMM College	4	1.5	0	0.0	4	1.5
Stanford University	18	11.2	0	0.0	18	11.2
Syracuse University	5	5.0	2	1.0	5	4.0
University of Florida	16	14.0	16	11.6	6	2.4
University of Michigan	4	2.8	4	2.8	0	0.0
University of Texas - Brownsville	4	2.5	4	2.5	0	0.0
University of Wisconsin-Milwaukee	6	5.3	6	5.3	0	0.0
<b>Total: Non-LIGO Laboratory</b>	<b>229</b>	<b>163.8</b>	<b>134</b>	<b>84.4</b>	<b>132</b>	<b>79.4</b>

*Sponsored by the National Science Foundation*



# The Observatories



LIGO Hanford



LIGO Livingston

*Photos: <http://www.ligo.caltech.edu>; <http://www.ligo-la.caltech.edu>*



# Inside





# Gravitational Waves

- Gravitation = spacetime curvature described by the metric tensor:  $ds^2 = g_{\mu\nu} dx^\mu dx^\nu$

- Weak Field Limit:  $g_{\mu\nu} = \eta_{\mu\nu} + h_{\mu\nu}$   
$$\left( \nabla^2 - \frac{1}{c^2} \frac{\partial^2}{\partial t^2} \right) \bar{h}^{\mu\nu} = 0$$

- TT Gauge:

$$h_{\mu\nu}^{TT} = \begin{pmatrix} 0 & 0 & 0 & 0 \\ 0 & h_+ & h_\times & 0 \\ 0 & h_\times & -h_+ & 0 \\ 0 & 0 & 0 & 0 \end{pmatrix} e^{2\pi i f t - i k z}$$



# Gravitational-wave Strain

$$c\Delta t = 2 \int_0^L \sqrt{1 + h_+} dx \cong 2L + h_+ L = 2L + \Delta L$$

$$h = \Delta L / L$$

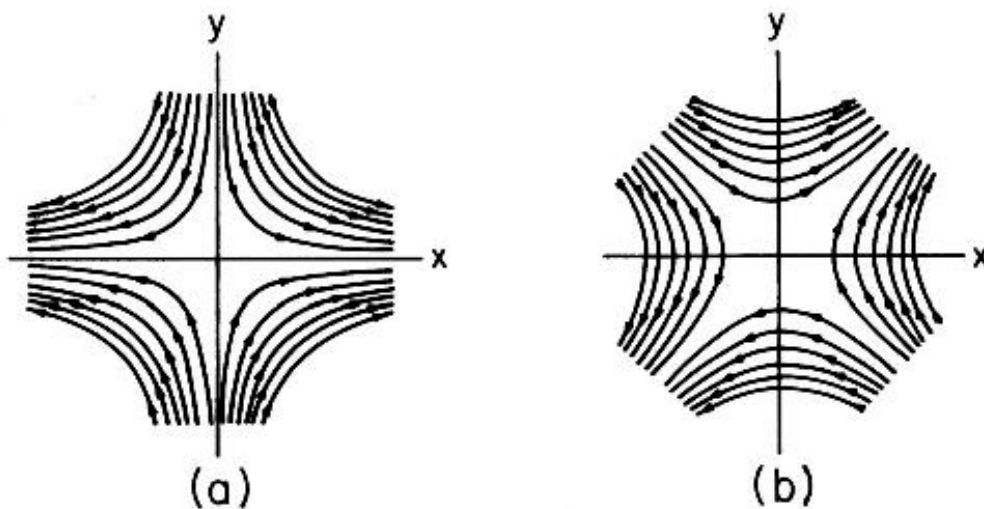
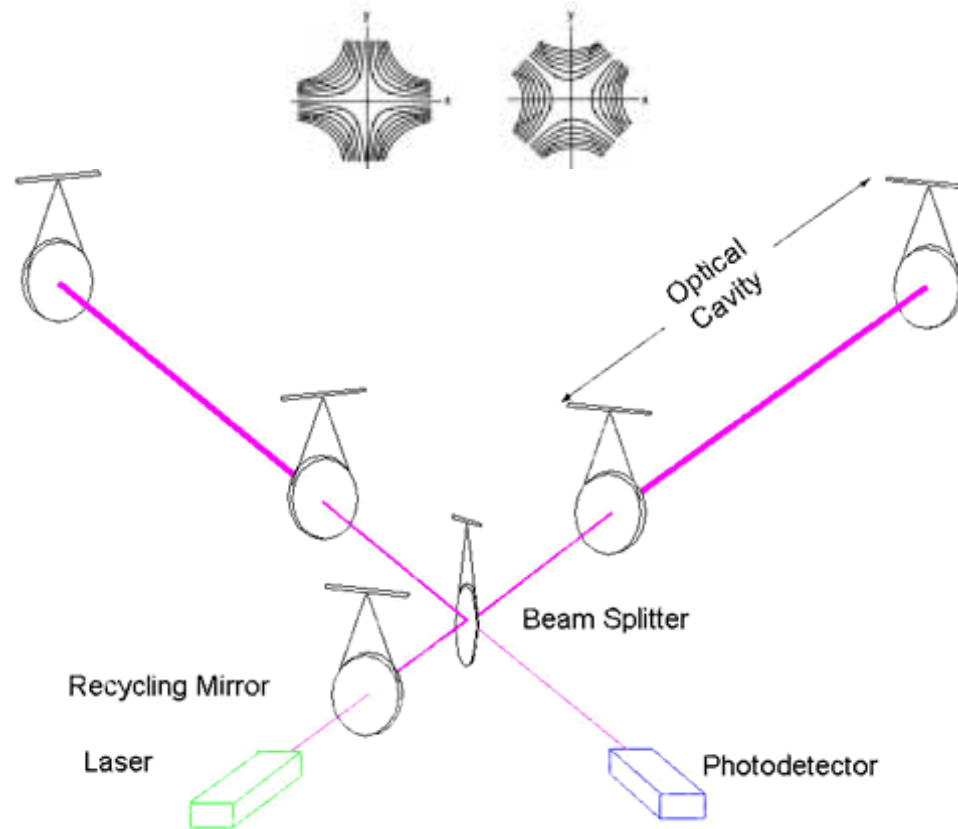


Figure 1. Direction of space deformation for a gravitational wave propagating along the z-axis, + polarization (a) and x polarization (b).



# How Does LIGO Work?

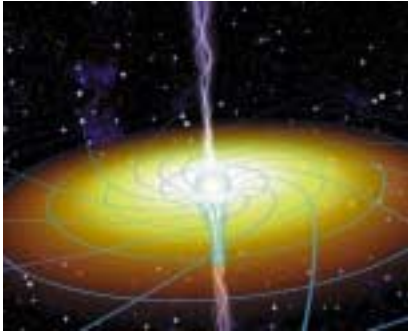
Gravitational-wave Strain:  $h = \Delta L / L$



**LIGO is a lab looking for GW's.**

**LIGO is an “ear” on the universe, listening for cosmic spacetime vibrations.**

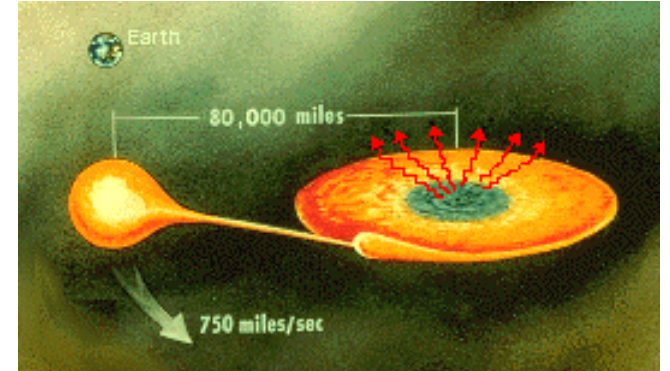
*Figures: K. S. Thorne gr-qc/9704042; D. Sigg LIGO-P980007-00-D*



Black Holes



Pulsars

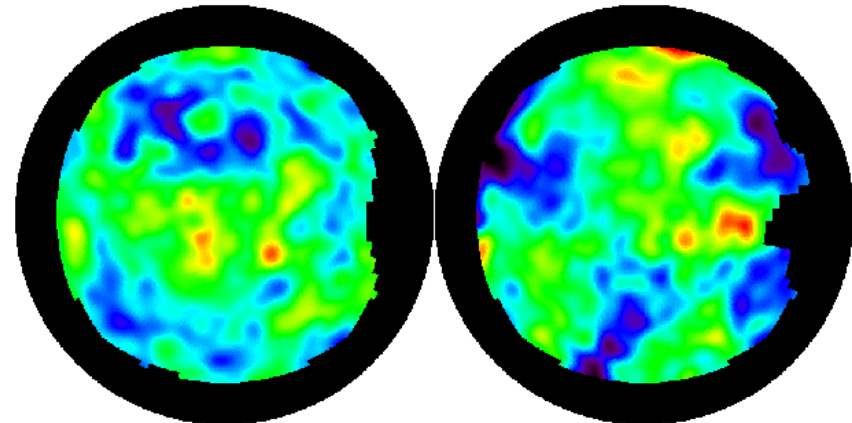


LMXBs

# Astrophysical Sources



Supernovae



North Galactic Hemisphere

South Galactic Hemisphere

Stochastic Background

Photos: <http://antwrp.gsfc.nasa.gov>; <http://imagine.gsfc.nasa.gov>





$$h = \Delta L / L \approx (G / c^4)(\ddot{Q} / r) \quad \text{“Newtonian” quadrupole formula.}$$

- **Stochastic** (limit  $\Omega_{\text{GW}}$ ; cosmic strings; BH from massive pop III stars:  $h = 10^{-23} - 10^{-21}$ )
- **Burst** (SN at distance of Virgo Cluster:  $h = 10^{-23} - 10^{-21}$ ; rate = 1/yr)
- **Inspiral** ( $h_{\text{max}} = 10^{-22}$  for NS-NS @ 200 Mpc; rate = 3/yr; NS-BH; BH-BH)
- **Periodic** ( $h = 10^{-25}$  for 10 ms pulsar with maximum ellipticity at 1 Kpc;  $h = 10^{-27}$  for 2 ms LMXB in equilibrium at 1 Kpc)



# Noise Curves

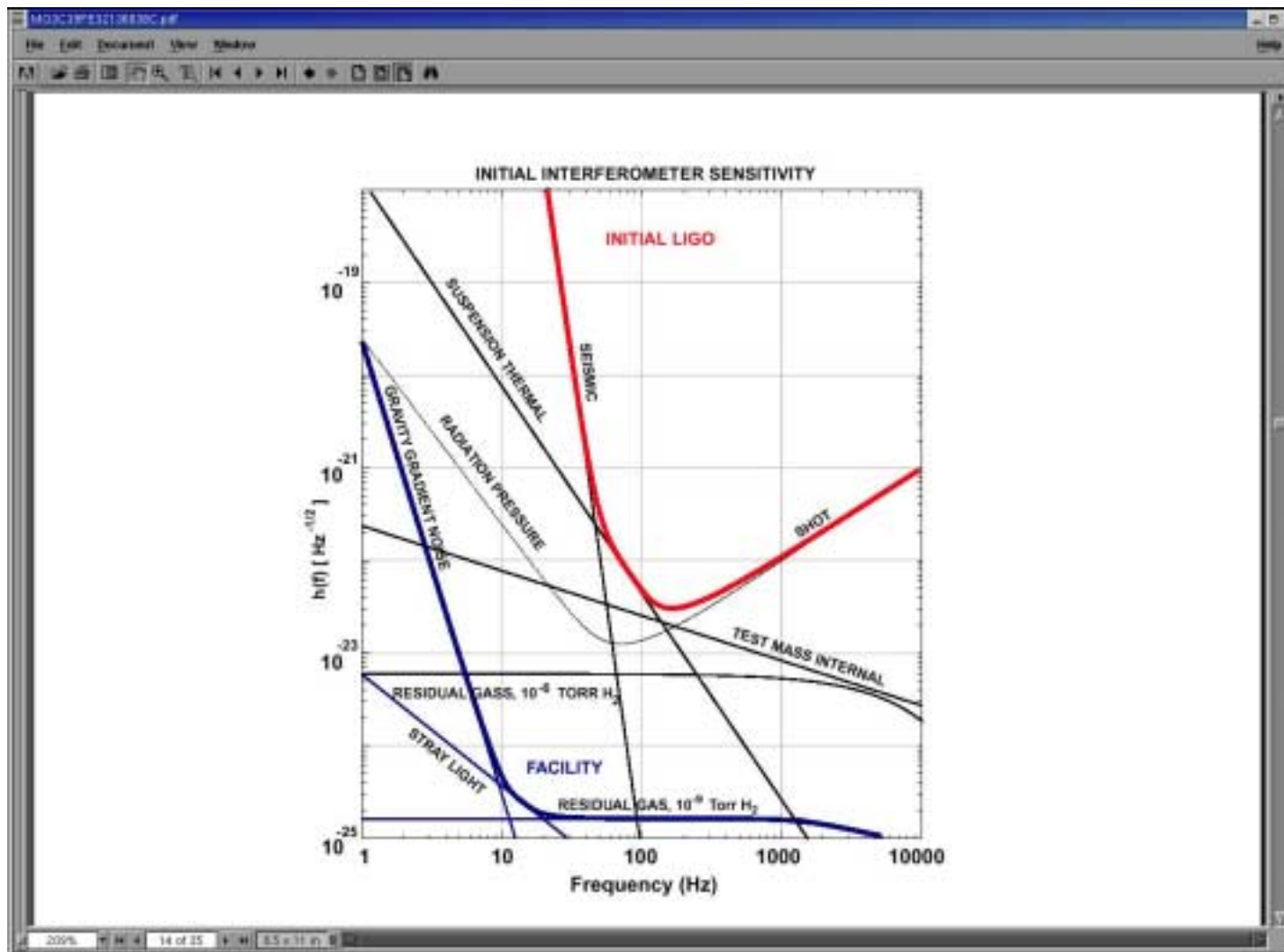


Figure: D. Sigg LIGO-P980007-00-D



# Signal to Noise Ratio

$$\frac{S}{N} \approx \frac{h\sqrt{T}}{\sqrt{\langle n^2(f_c) \rangle}}$$

- **$h$  = signal amplitude**
- **$T$  = observation time or duration of signal or period of the characteristic frequency of the signal.**
- **$n^2$  = power spectrum of the noise**



# Sensitivity Curves

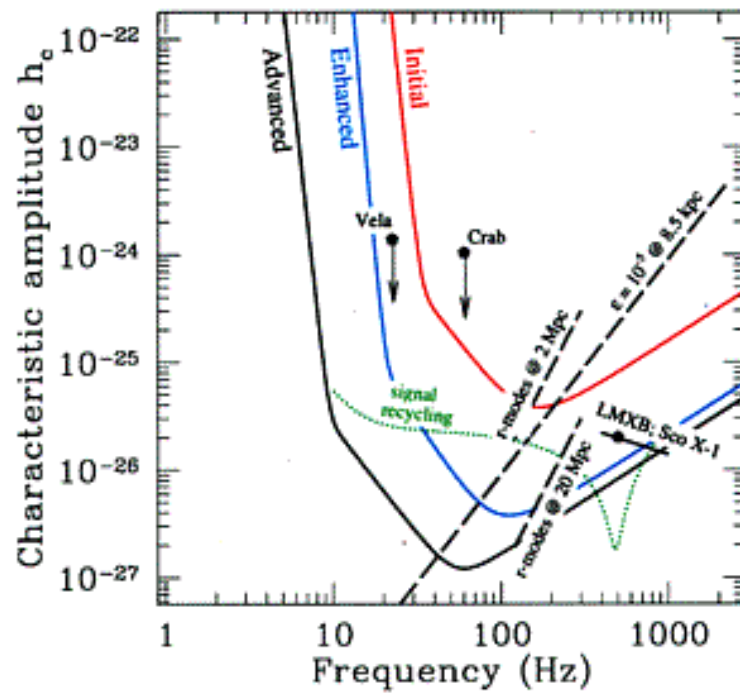
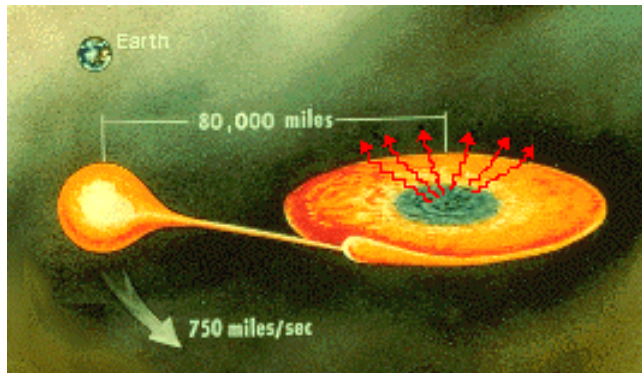
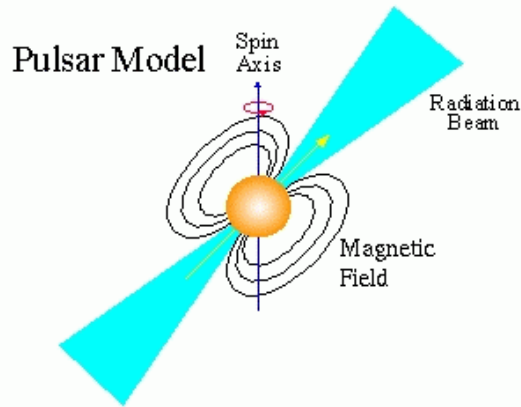


Figure: Brady ITP seminar summer 2000



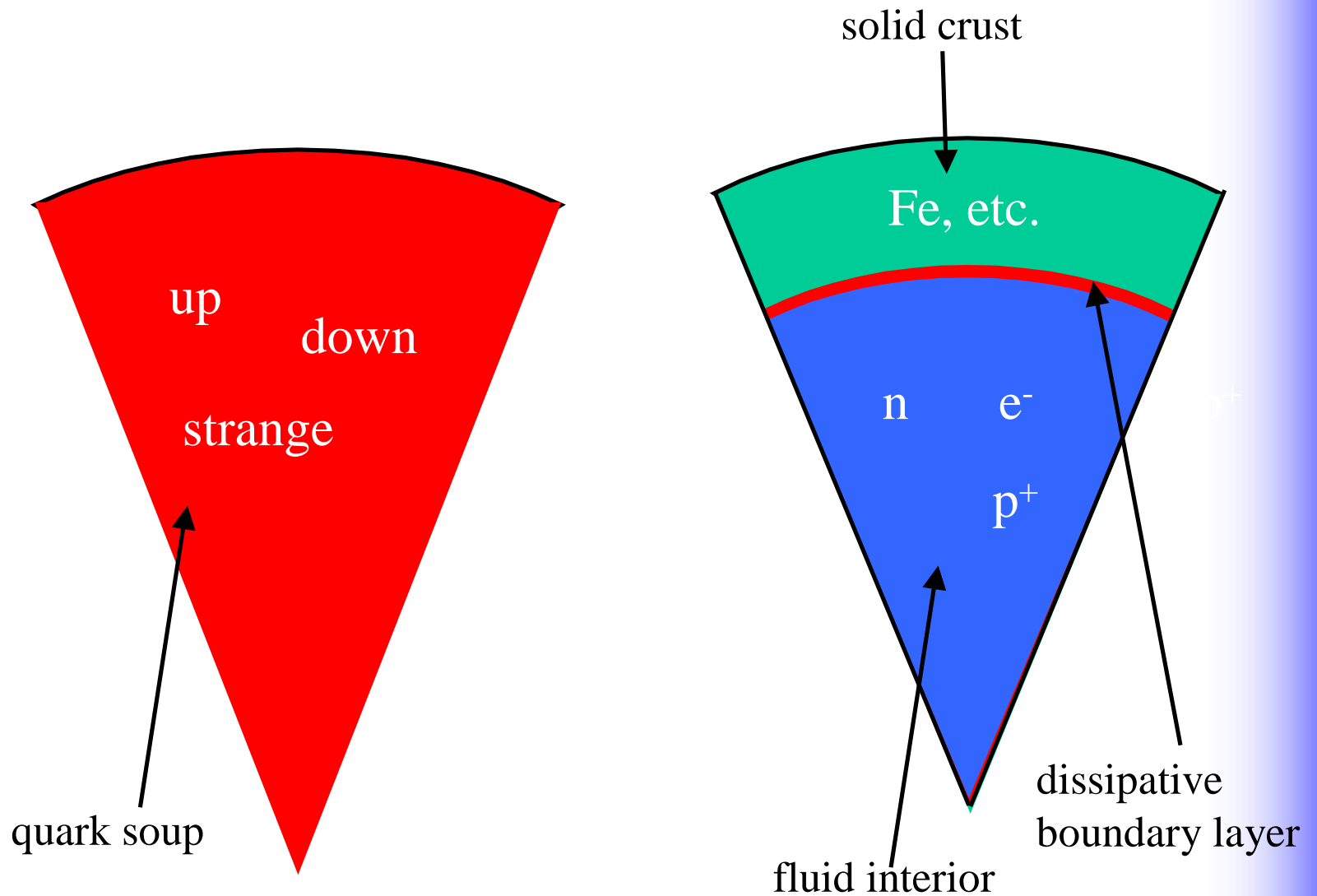
# Known Possible Periodic Sources



LMXBs

- Are neutron stars: the sun compress to size of city. Compact ( $2GM/Rc^2 \sim .2$ ) and ultra dense ( $10^{14} \text{ g/cm}^3$ ).
- Are composed of (superfluid) **neutrons**, (superconducting) protons, electrons, + exotic particles (e.g., hyperons) or **strange** stars composed of an even more exotic up, down, and strange quark soup.
- Spin Rapidly ( $\sim .1 \text{ Hz}$  to  $642 \text{ Hz}$  i.e., within the LIGO band.)

# Neutron (Strange) Star Models



*Courtesy Justin Kinney*



## Periodic sources emit GWs due to...

- Rotation about nonsymmetry axis
- Strain induced asymmetry:  $\varepsilon = \frac{I_1 - I_2}{I}$
- Accretion induced emission
- Unstable oscillation modes



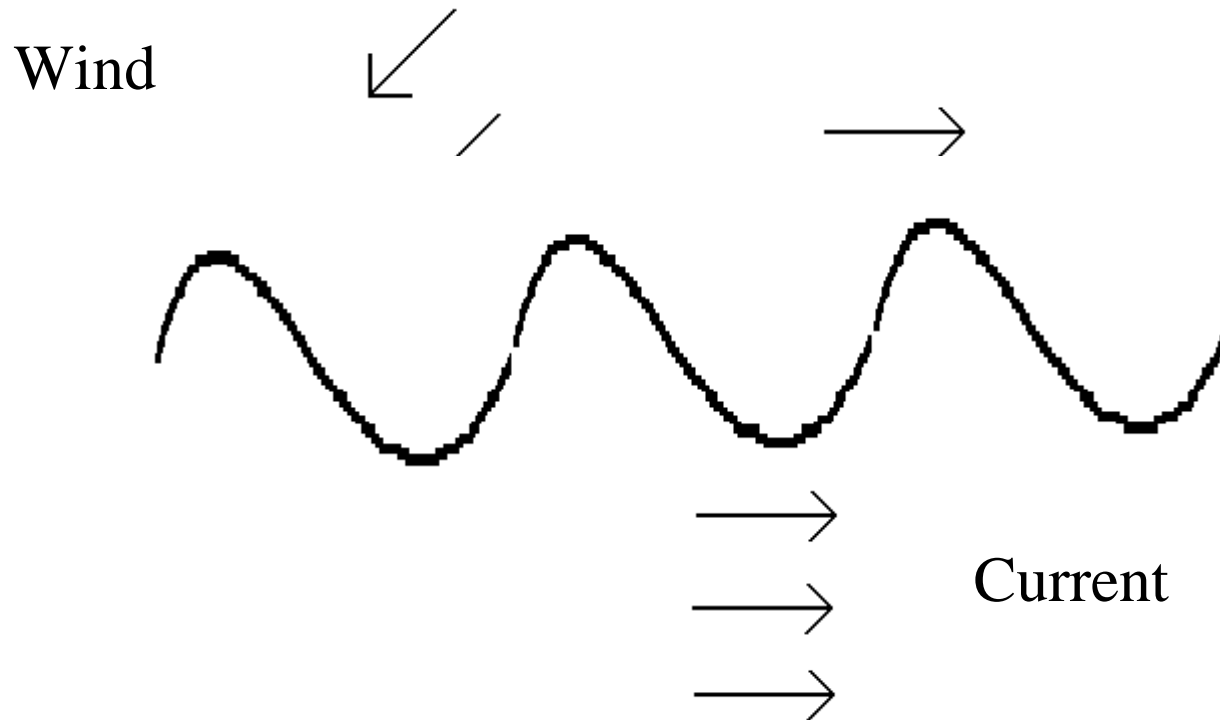
# Gravitational-radiation Driven Instability of Rotating Stars

- GR tends to drive all rotating stars unstable!
- Internal dissipation suppresses the instability in all but very compact stars.



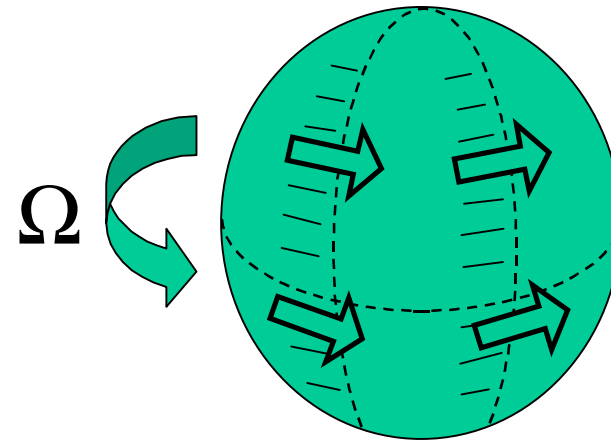


# Ocean Wave Instability

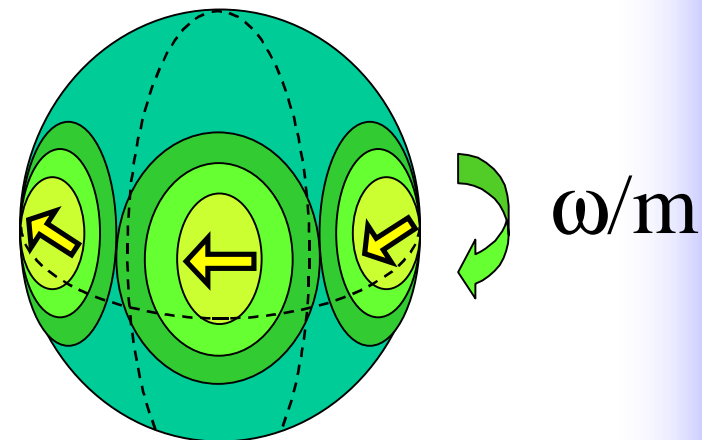


# Perturbations in Rotating Neutron Stars

- Neutron star rotates with angular velocity  $\Omega > 0$ .
- Some type of “wave” perturbation flows in opposite direction with phase velocity  $\omega/m$ , as seen in rotating frame of star.
- Perturbations create rotating mass and momentum multipoles, which emit GR.



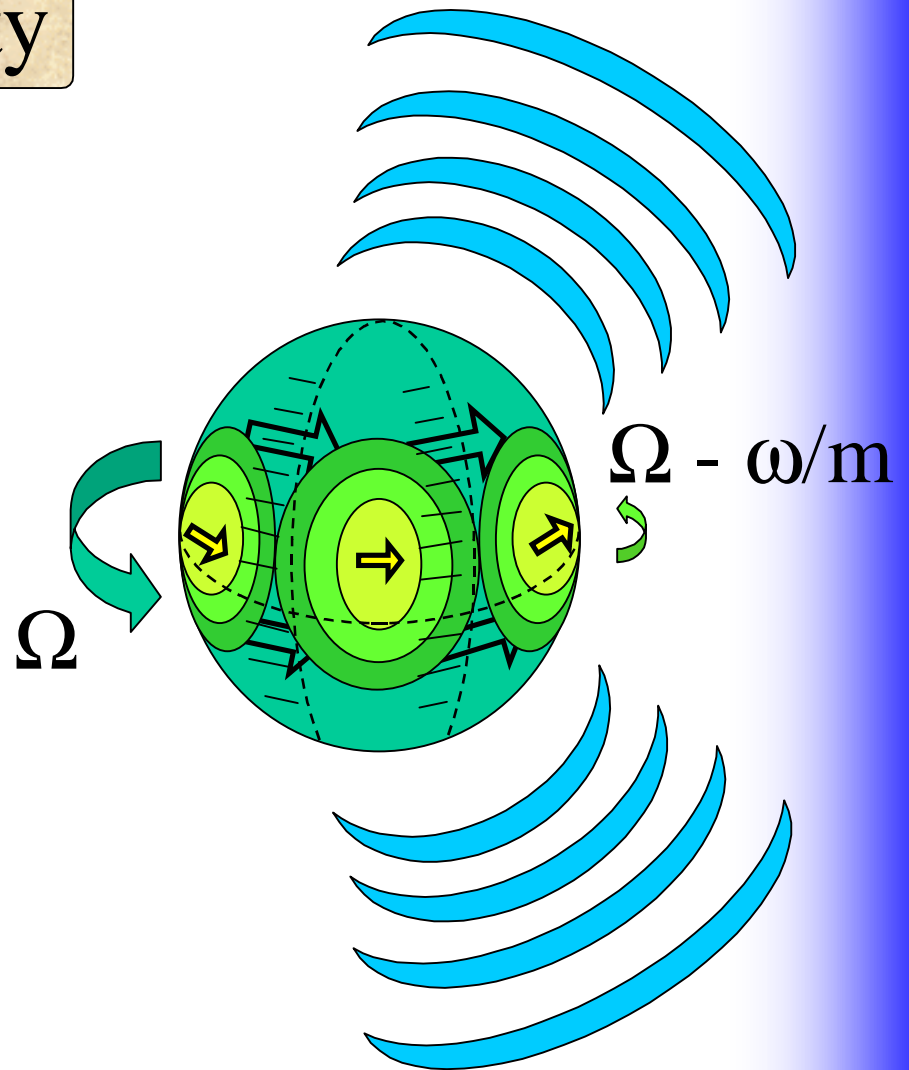
Rotating neutron star.



Perturbations in rotating frame.

# GR Causes Instability

- If  $\Omega - \omega/m > 0$ , star “drags” perturbations in opposite direction.
- GR carries away positive angular momentum.
- This adds negative angular momentum to the perturbations.
- This *increases* their amplitude!



Star drags perturbations in opposite direction. GR drives mode instability.

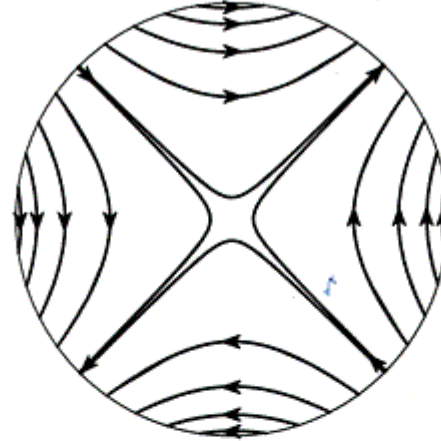


# The R-modes

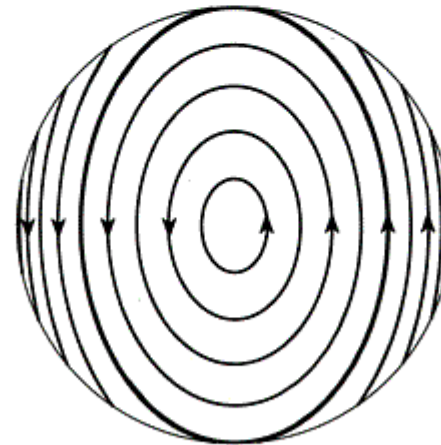
- The r-modes corresponds to oscillating flows of material (currents) in the star that arise due to the Coriolis effect. The r-mode frequency is proportional to the angular velocity,  $\Omega$ .
- The current pattern travels in the azimuthal direction around the star as  $\exp(i\omega t + im\varphi)$
- For the  $m = 2$  r-mode:
  - Phase velocity in the corotating frame:  $-1/3 \Omega$
  - Phase velocity in the inertial frame:  $+2/3 \Omega$

## Flow Pattern for the $m = 2$ r-mode

Polar View

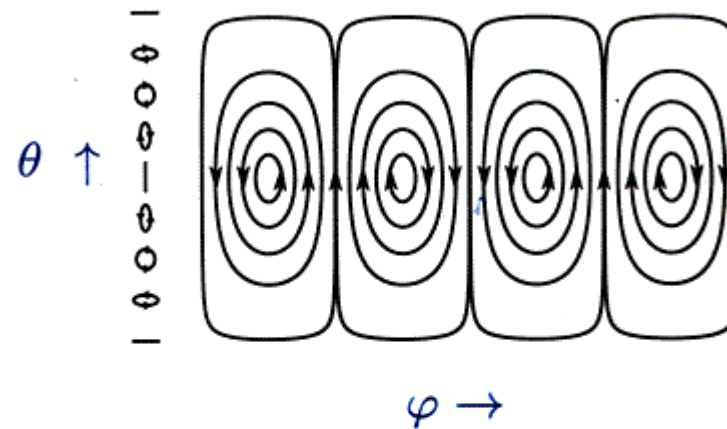


Equatorial View



*Courtesy Lee Lindblom*

## Fluid Motion in the $m = 2$ r-mode



- The flow pattern is shown along with the small elliptical paths (on the left) of individual fluid elements. The flow pattern moves (to the left) past the fluid particles as the mode evolves.

*Courtesy Lee Lindblom*



# R-mode Instability Calculations

- Gravitation radiation tends to make the r-modes grow on a time scale  $\tau_{\text{GR}}$
- Internal friction (e.g., viscosity) in the star tends to damp the r-modes on a time scale  $\tau_{\text{F}}$
- The shorter time scale wins:
  - $\tau_{\text{GR}} < \tau_{\text{F}}$  : Unstable!
  - $\tau_{\text{GR}} > \tau_{\text{F}}$  : Stable!



# Key Parameters to Understanding the R-mode Instability

- Critical angular velocity for the onset of the instability
- Saturation amplitude





- The Shear Force:

$$F = \eta \frac{\left(\frac{\Delta v_y}{\Delta x}\right)_b - \left(\frac{\Delta v_y}{\Delta x}\right)_a}{\Delta x} A \Delta x,$$

where  $\eta$  is the viscosity.

- Newton's 2nd Law:

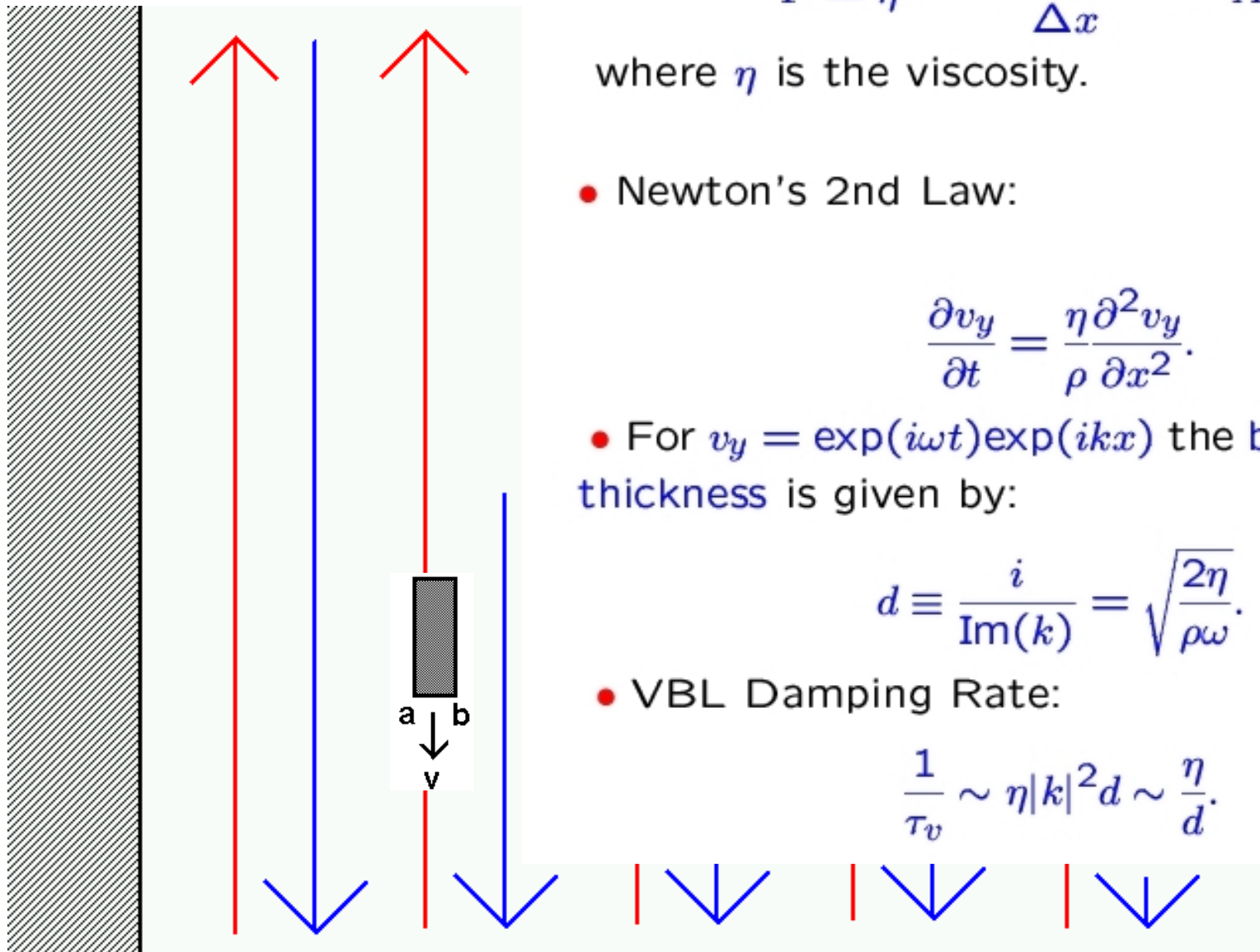
$$\frac{\partial v_y}{\partial t} = \frac{\eta}{\rho} \frac{\partial^2 v_y}{\partial x^2}.$$

- For  $v_y = \exp(i\omega t)\exp(ikx)$  the boundary layer thickness is given by:

$$d \equiv \frac{i}{\text{Im}(k)} = \sqrt{\frac{2\eta}{\rho\omega}}.$$

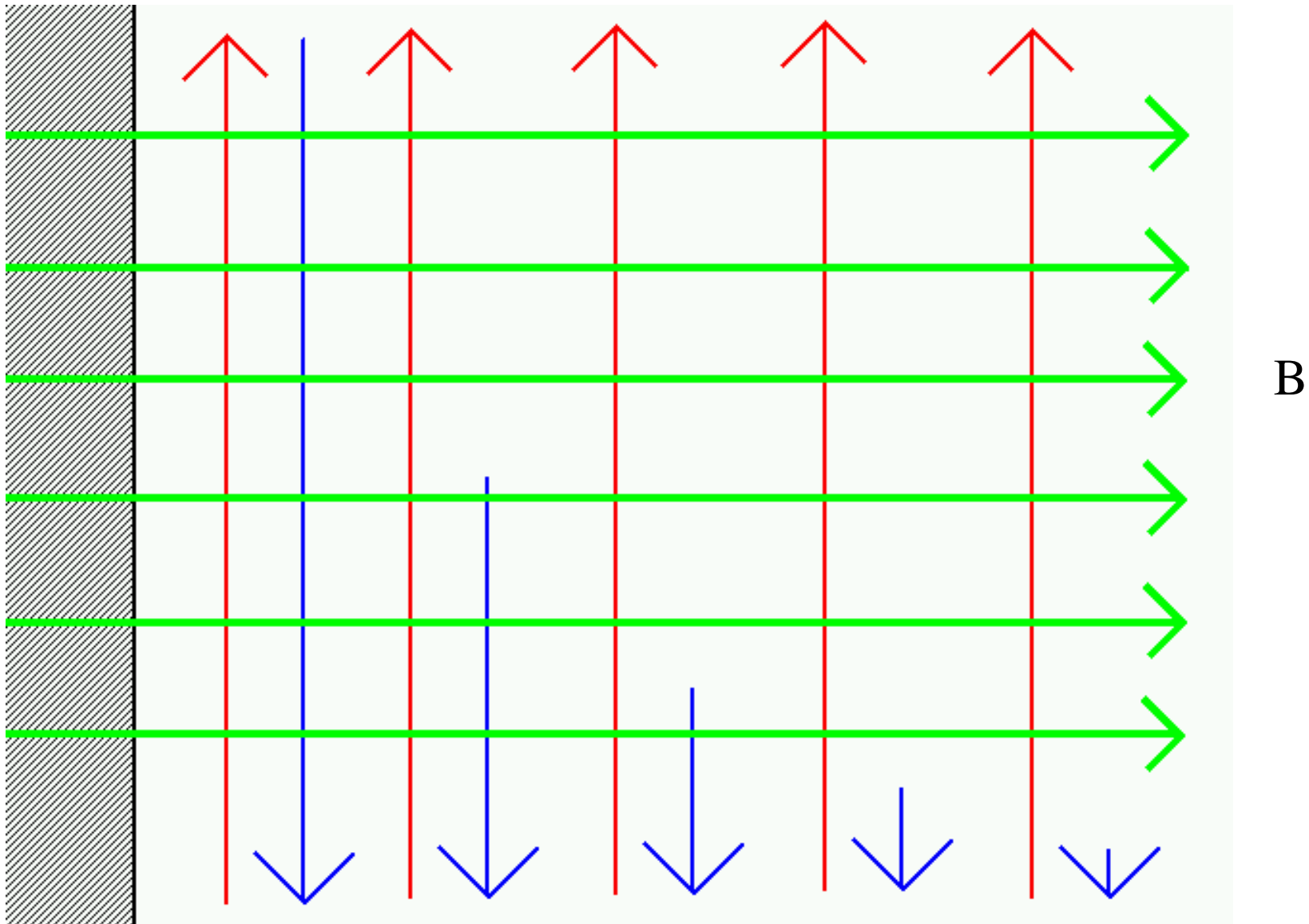
- VBL Damping Rate:

$$\frac{1}{\tau_v} \sim \eta |k|^2 d \sim \frac{\eta}{d}.$$



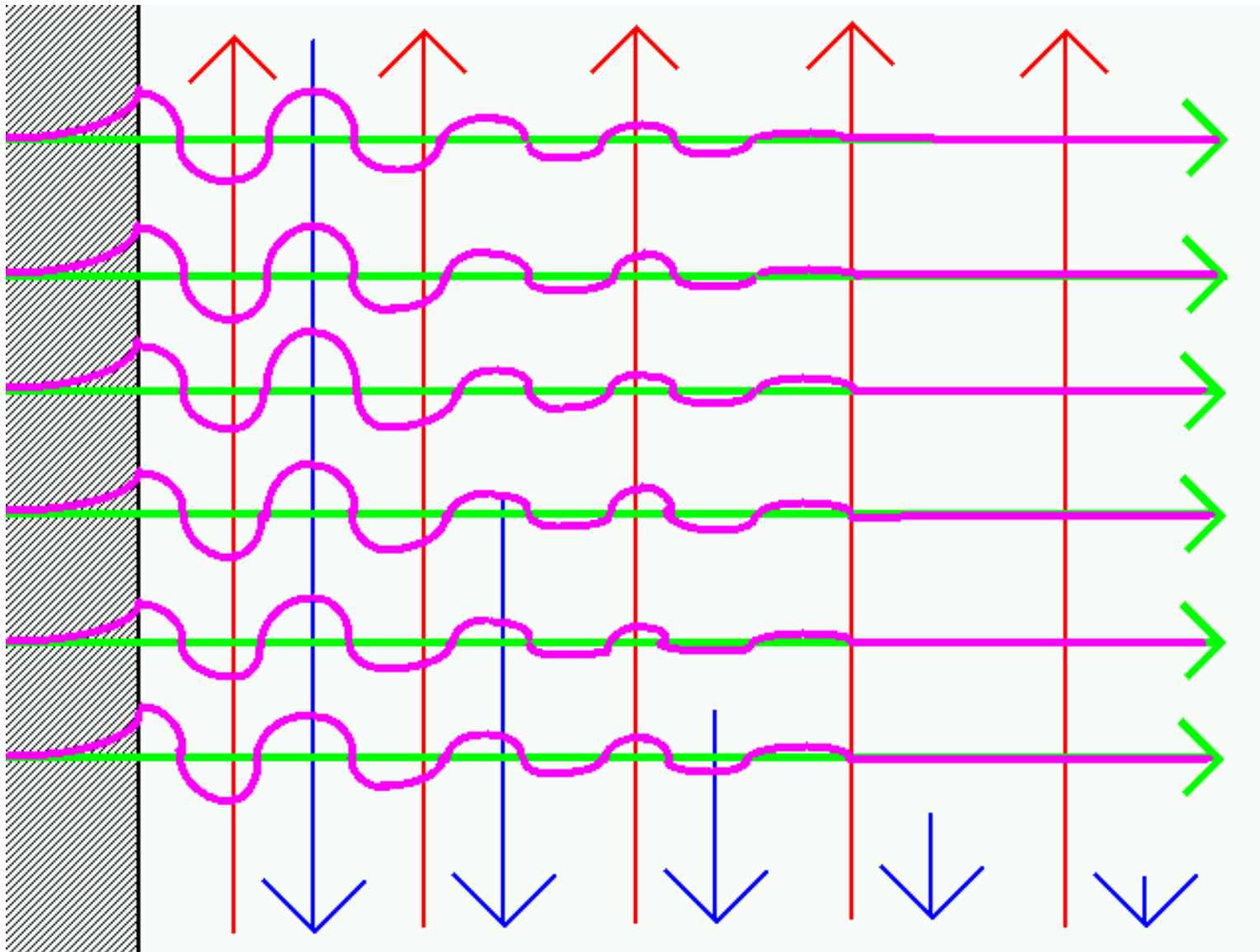


# Add Magnetic Field...





# Magneto-viscous Boundary Layer With Alfven Waves





- Equation for the critical angular velocity:

$$\tau_{GR} = \tau_v.$$

- Gravitational-radiation growth rate for the  $m = 2$  r-modes:

$$\frac{1}{\tau_{GR}} = 0.24 \text{ s}^{-1} \left( \frac{\Omega}{\Omega_o} \right)^6,$$

where

$$\Omega_o = \sqrt{\pi G \bar{\rho}},$$

$$\Omega_{\max} \cong \frac{2}{3} \Omega_o,$$

- Magneto-viscous boundary layer damping rate for the  $m = 2$  r-modes:

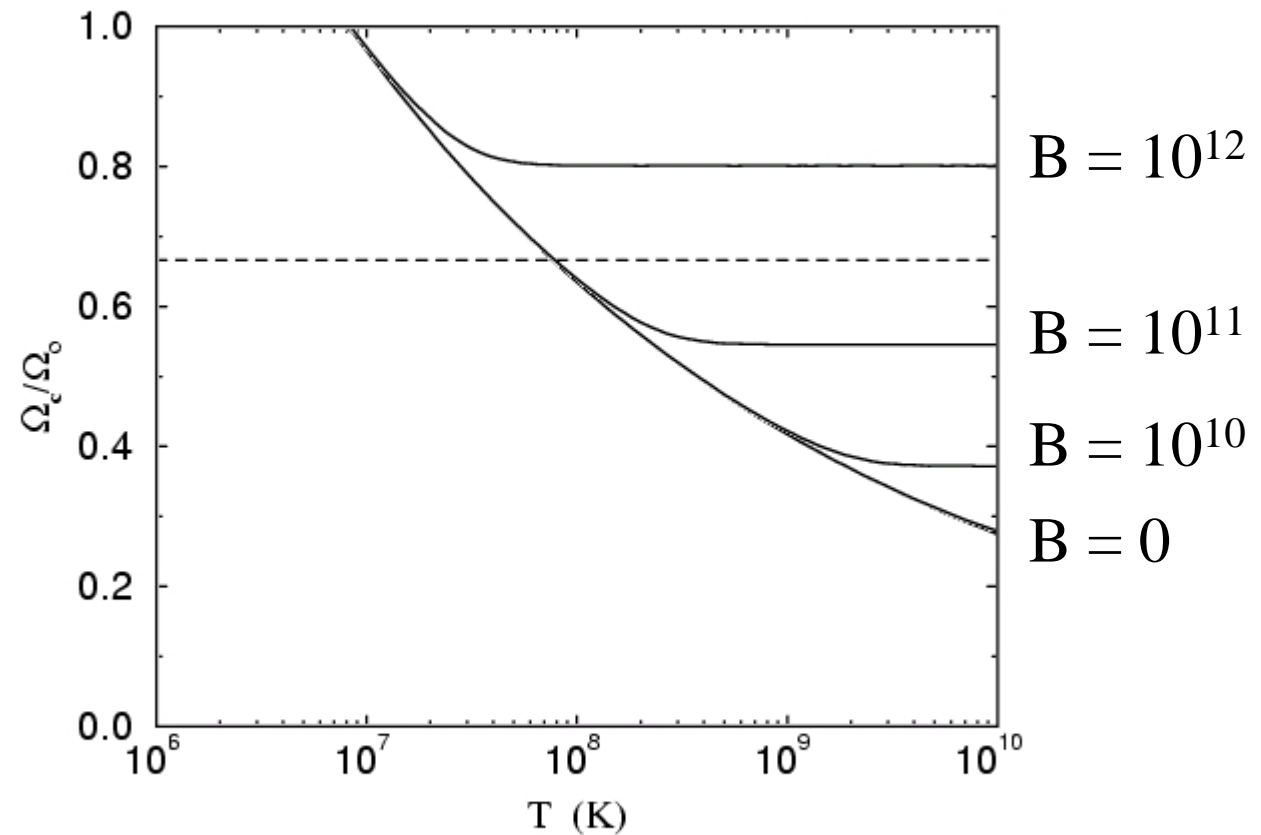
$$\frac{1}{\tau_v} \sim \eta |k|^2 d \sim \eta \frac{d}{\lambda^2} \sim 0.062 \text{ s}^{-1} B_{12}.$$

- Critical angular velocity:

$$\frac{\Omega_c}{\Omega_o} = 0.8 B_{12}^{1/6}.$$



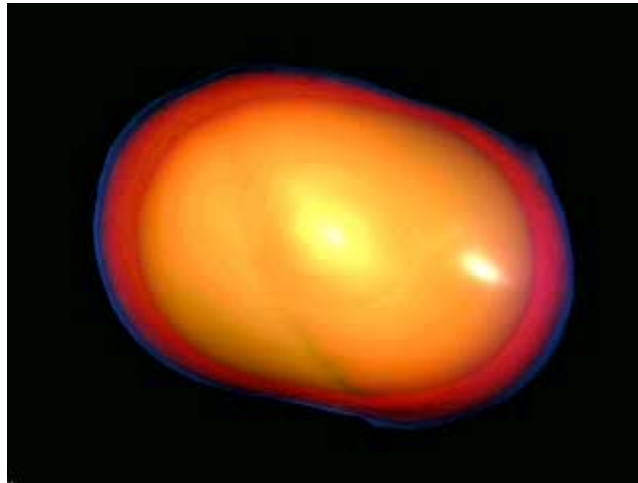
# MVBL Critical Angular Velocity



*Mendell 2001, Phys Rev D64 044009; gr-qc/0102042*



# R-mode Movie



See: <http://www.cacr.caltech.edu/projects/hydrigo/rmode.html>

Lee Lindblom, Joel E. Tohline and Michele Vallisneri (2001), Phys. Rev. Letters 86, 1152-1155 (2001). R-modes in newborn NS are saturated by breaking waves.

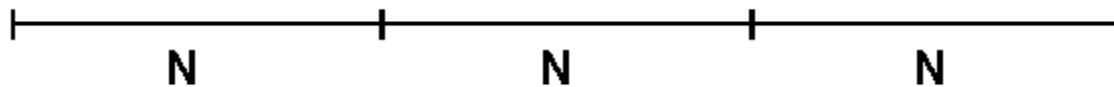
Computed using Fortran 90 code linked with the MPI library on CACR's HP Exemplar V2500.

Owen and Lindblom gr-qc/0111024: r-modes produce 100 s burst with  $f \sim 940-980$  Hz and optimal SNR  $\sim 1.2-12$  for  $r = 20$  Mpc and enhanced LIGO.



# Basic Detection Strategy

- Coherently add the signal
- Signal to noise ratio  $\sim \sqrt{T}$
- Can always win as long as
  - Sum stays coherent
  - Understand the noise
  - Do not exceed computational limits



$$X_b = \sum_{a=0}^{NM-1} x_a A_a e^{-2\pi i \Phi_{ab}}$$



# Amplitude Modulation

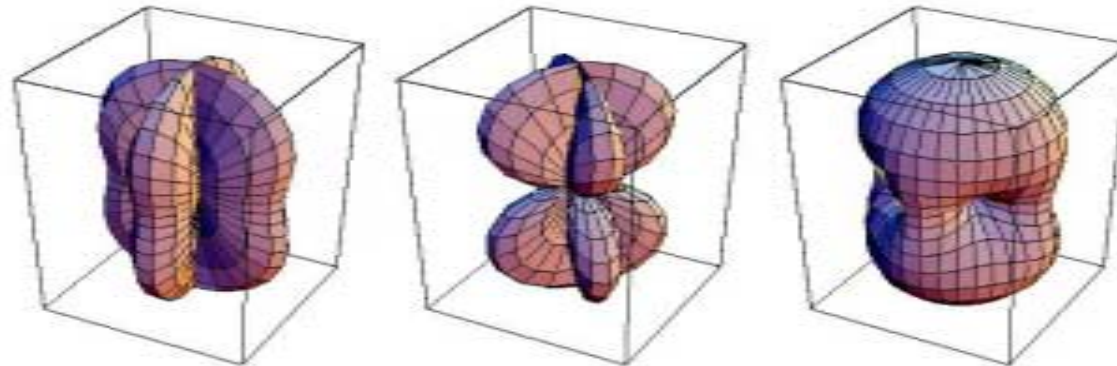


Figure 9. Antenna response function for an interferometric gravitational wave detector. The interferometer is placed at the center of the surrounding box with Michelson arms oriented along the horizontal axes. The distance from a point of the plot surface to the center of the box is a measure for the gravitational wave sensitivity in this direction. The plot to the left is for + polarization, the middle one for  $\times$  polarization and the right one for unpolarized waves.

$$h(t) = \hat{x} \cdot (Mh^{TT} M^t) \cdot \hat{x} - \hat{y} \cdot (Mh^{TT} M^t) \cdot \hat{y}$$

$$h(t) = h_+ [0.5(1 + \cos^2 \theta) \cos 2\varphi \cos 2\psi - \cos \theta \sin 2\varphi \sin 2\psi]$$

$$+ h_\times [0.5(1 + \cos^2 \theta) \cos 2\varphi \sin 2\psi - \cos \theta \sin 2\varphi \cos 2\psi]$$

Figure: D. Sigg LIGO-P980007-00-D





# Phase Modulation

$$\Phi = \int_0^t f_0 \left(1 + \sum_n f_n t^n\right) \left(1 + \frac{\vec{v}}{c} \cdot \hat{n}\right) dt$$

- The phase is modulated by the intrinsic frequency evolution of the source and by the Doppler effect due to the Earth's motion
- The Doppler effect can be ignored for

$$T \leq 5.5 \times 10^3 \sqrt{\frac{300 \text{ Hz}}{f_0}} \text{ sec.}$$



# DeFT Algorithm

$$X_b = \sum_{\alpha=0}^{M-1} \sum_{j=0}^{N-1} x_{\alpha j} A_{\alpha} e^{-2\pi i \Phi_{\alpha j b}}$$

$$x_{\alpha j} = \sum_{k=0}^{N-1} X_{\alpha j}^{SFT} e^{-2\pi i \Phi_{\alpha b}}$$

$$X_b = \sum_{\alpha=0}^{M-1} A_{\alpha} Q_{\alpha b} \sum_{k=0}^{N-1} X_{\alpha k}^{SFT} P_{\alpha k b}$$

*AEI: Schutz & Papa gr-qc/9905018; Williams and Schutz gr-qc/9912029;  
Berukoff and Papa LAL Documentation*



## Taylor expand the phase

$$\Phi_{\alpha j b} = \Phi_{\alpha, 1/2, b} + f_{\alpha, 1/2, b} (t_{\alpha j} - t_{\alpha, 1/2})$$

$$P_{\alpha k b} = \frac{\sin u_{\alpha k b}}{u_{\alpha k b}} - i \frac{1 - \cos u_{\alpha k b}}{u_{\alpha k b}}$$

$$Q_{\alpha b} = e^{i v_{\alpha b}}$$

$$u_{\alpha k b} = 2\pi \left( \frac{T}{M} f_{\alpha, 1/2, b} - k \right)$$

$$v_{\alpha b} = -2\pi \left( \Phi_{\alpha, 1/2, b} - \frac{T}{2M} f_{\alpha, 1/2, b} \right)$$



# Advantages of DeFT Code

- $P_{\alpha kb}$  is peaked. Can sum over only 16  $k$ 's
- Complexity reduced from  $O(MN \times \text{number of phase models})$  to  $O(MN \log_2 N + M \times \text{number of phase models})$ .
- Unfortunately, number phase models increased by factor of  $M/\log_2 MN$  over FFT of modulated data. FFT is  $O(MN \log_2 MN \times \text{number of phase models}/MN)$ .
- But memory requirements much less than FFT, and easy to divide DeFT code into frequency bands and run on parallel computing cluster.
- Need  $10^{10} - 10^{20}$  phase models, depending on frequency band & number of spin down parameters, for no more than 30% power loss due to mismatch.



# Basic Confidence Limit

- Probability stationary white noise will result in power greater than or equal to  $P_f$ :

$$1 - \alpha = e^{-P_f / P_n}$$

- Threshold needed so that probability of false detection =  $1 - \alpha$ .

$$P_f / P_n > \ln[N_p / (1 - \alpha)]$$



# Maximum Likelihood Estimator

$$h = F_+ h_+ + F_\times h_\times$$

$$S = \frac{4}{T} \frac{A|F|^2 + B|G|^2 - 2C \operatorname{Re}(FG^*)}{D}$$

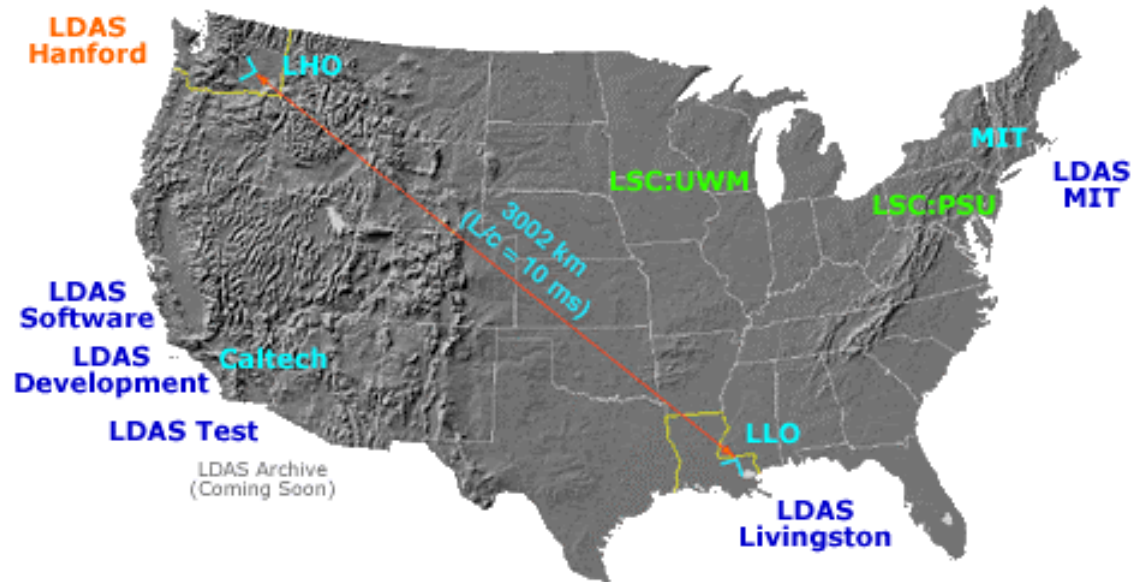
$$p = \frac{1}{\pi^2 D} e^{-S}$$

$$F = \sum_{a=0}^{NM-1} x_a f_a e^{-2\pi i \Phi_{ab}}, \quad G = \sum_{a=0}^{NM-1} x_a g_a e^{-2\pi i \Phi_{ab}}$$

$$f = F_+ \cos 2\Psi - F_\times \sin 2\Psi, \quad g = F_+ \sin 2\Psi + F_\times \cos 2\Psi$$



# LDAS = LIGO Data Analysis Systems





# LDAS Hardware

**14.5 TB Disk Cache**



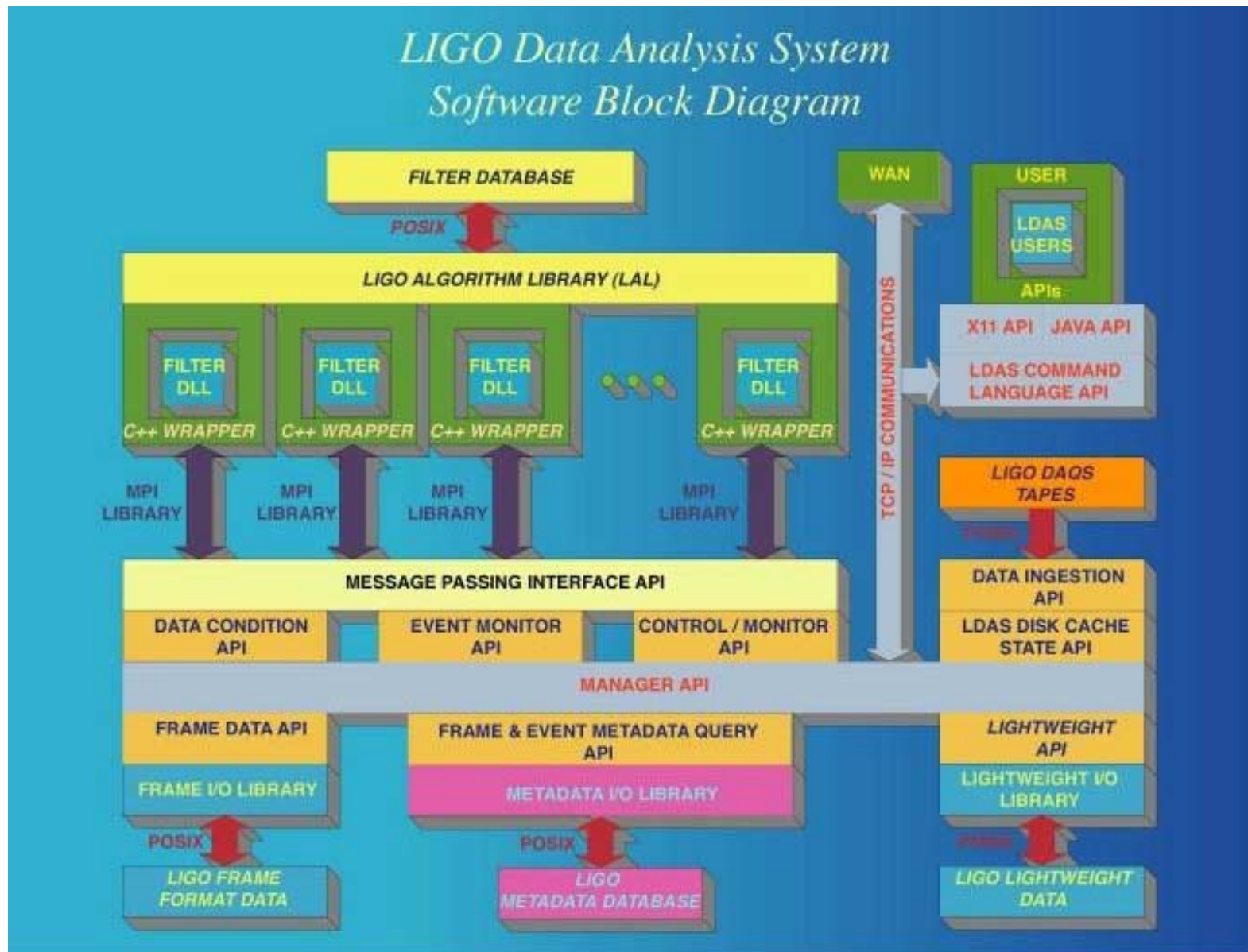
**Beowulf Cluster**







# LDAS Software





# Interface to the Scientist

